

# Influence of stacking towards the aqueous proton penetration behavior across two-dimensional graphtetrayne

## Supporting Information

*Zhixuan Ying<sup>1</sup>; Yushuan Gao<sup>1</sup>; Yongpeng Meng<sup>1</sup>; Yonghong Cheng<sup>1</sup>; Le Shi<sup>\*,1</sup>*

1. State key Laboratory of Electrical Insulation and Power Equipment, Center of Nanomaterials for Renewable Energy, School of Electrical Engineering, Xi'an Jiaotong University, Xi'an 710049, China

Table S1 Interlayer distance between double-layer G4s after NPT process

<b>Initial interlayer distance/ Å</b>	<b>Interlayer Distance (AA) /Å</b>	<b>Interlayer Distance (AB)/ Å</b>
2.5	3.2648±0.2619	3.4785±0.2875
3.5	3.3369±0.3287	3.6705±0.1995
6	3.4831±0.2756	3.4657±0.2536
8	3.6412±0.2905	3.3884±0.3118

Table S2 Misplacement in x and y directions for AA-stacked double-layer G4s after NPT process

<b>Initial interlayer distance (AA)/Å</b>	<b>D<sub>x</sub>/Å</b>	<b>D<sub>y</sub>/Å</b>
2.5	1.586295	1.872736
3.5	1.706644	-1.842920
6	-1.790785	1.336426
8	-0.336938	2.152781

Table S3 Misplacement in x and y directions for AB-stacked double-layer G4s after NPT process

<b>Initial interlayer distance (AB)/ Å</b>	<b>D<sub>x</sub>/Å</b>	<b>D<sub>y</sub>/Å</b>
2.5	1.615270	-1.337390
3.5	1.010026	-1.034090
6	0.863822	1.294675
8	0.034599	-2.543637

Table S4 Interlayer distance between AAA-stacked triple-layer G4s after NPT process

<b>Initial interlayer distance (AAA)/Å</b>	<b>Layer Distance_12 /Å</b>	<b>Layer Distance_23 /Å</b>
2.5	3.6172±0.3297	3.5317±0.3657
3.5	3.4219±0.2669	3.5659±0.3445
6	3.4880±0.1905	3.5532±0.3146
8	3.5267±0.2729	3.6215±0.2221

Table S5 Interlayer distance between ABA-stacked triple-layer G4s after NPT process

<b>Initial interlayer distance (ABA)/Å</b>	<b>Layer Distance_12 /Å</b>	<b>Layer Distance_23 /Å</b>
2.5	3.5944±0.2277	3.4735±0.3182
3.5	3.5477±0.2252	3.6784±0.2638
6	3.6177±0.2745	3.5992±0.2160
8	3.5103±0.2179	3.7227±0.2583

Table S6 Misplacement in x and y directions for AAA-stacked triple-layer G4s after NPT process

<b>Initial interlayer Distance (AAA)/Å</b>	<b>D<sub>x</sub>/Å</b>	<b>D<sub>y</sub>/Å</b>
2.5	-0.120770	1.889484
	-0.741793	-2.059277
3.5	0.656403	2.176183
	-1.681395	0.929210
6	-0.192795	1.803464
	0.569046	-1.775180
8	0.740805	1.975794
	-0.648285	-1.239815

Table S7 Misplacement in x and y directions for ABA-stacked triple-layer G4s after NPT process

<b>Initial interlayer Distance (ABA)/Å</b>	<b>D<sub>x</sub>/Å</b>	<b>D<sub>y</sub>/Å</b>
2.5	-0.531736	-1.442914
	-0.216179	2.041926
3.5	0.766084	-1.999929
	-1.184297	1.143129
6	-0.305837	-1.580782
	-1.241465	1.619881
8	-0.662102	1.304054
	1.112363	-0.480463

Table S8 Simulation box length in z direction after NPT process

<b>Number of G4 layers</b>	<b>L<sub>z</sub>/Å</b>
1	50.448973
2	54.565490
3	60.408641

We suspected the squeezing-out of water molecules and the eventual approach of multilayer G4s may result from the minority of water molecules positioned within the G4s in the initial geometry. Therefore, models with more water molecules depositing interlayer were built and underwent identical NPT and NVT process (Figure S21). As shown in Figure S22-23, these cases took more time to converge. For double-layer cases, they reveal the same geometry at the end of NPT process as the models with initially minority water molecules. But for cases of triple-layer whose initial interlayer distance is 8 Å, several water molecules are kept interlayer and the G4 layers are not parallelly stacked, as shown in Figure S24. According to further comparison about the total energy of each ensemble shown in Table S9, ensembles with no water interlayer reveal lower energy. Thus, the geometry with water molecules interlayer can be regarded as metastable and the parallelly stacking pattern of multilayer G4s is further verified to be a stable configuration in aqueous environment.

Table S9 Mean energy of NVT ensembles of AAA8 and ABA8

<b>Interlayer Distance/Å</b>	<b>Origin/kCal mole<sup>-1</sup></b>	<b>More water molecules/kCal mole<sup>-1</sup></b>
AAA8	-361446.9024	-361268.0182
ABA8	-361442.2966	-361314.8077

The area-normalized proton conductance of single- and double-layer G4 is calculated from the energy barriers of proton penetration using the Nernst-Einstein relation:

$$\sigma_{H^+}^* = \frac{F^2}{RT} D_{H^+} C_{H^+} / d$$

where  $F$  is the Faraday constant,  $R$  is the ideal gas constant,  $T$  is temperature,  $C_{H^+}$  is the concentration of proton and  $d$  is the membrane thickness.  $D_{H^+}$  is the diffusion coefficient of proton, which can be estimated by Einstein-Smoluchowski equation:

$$D_{H^+} = \frac{l^2}{\kappa\tau_D}$$

where  $l$  is the mean step distance, and  $\kappa$  is the one-dimensional random-walk constant ( $\kappa=2$ ).  $\tau_D$  is the mean time between successive steps estimated by:

$$\tau_D = \nu_0^{-1} \exp\left(\frac{\Delta G}{k_B T}\right)$$

where  $k_B$  is the Boltzmann Constant,  $\nu_0$  is the thermal frequency with  $\nu_0 = k_B T / h$ ,  $h$  is the Planck constant, and  $\Delta G$  is the effective Gibbs free energy of activation for proton diffusion.

Here we take the length of vacuum phase at the interphase as the membrane thickness and the mean step distance for proton penetration (filled areas shown in Figure S16). The values are 6.34Å, 10.21Å and 14.83 Å for single-, double- and triple-layer G4, respectively. For proton conduction at room temperature with proton concentration of 1M, the calculated proton conductance are  $8.57 \times 10^6$  S cm<sup>-2</sup>,  $2.22 \times 10^7$  S cm<sup>-2</sup> and  $5.79 \times 10^{-21}$  S cm<sup>-2</sup> for single-, double- and triple-layer G4, respectively.

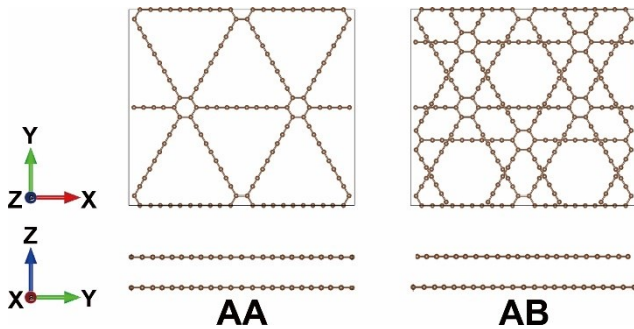


Figure S1 Initial stack geometry of double-layer G4

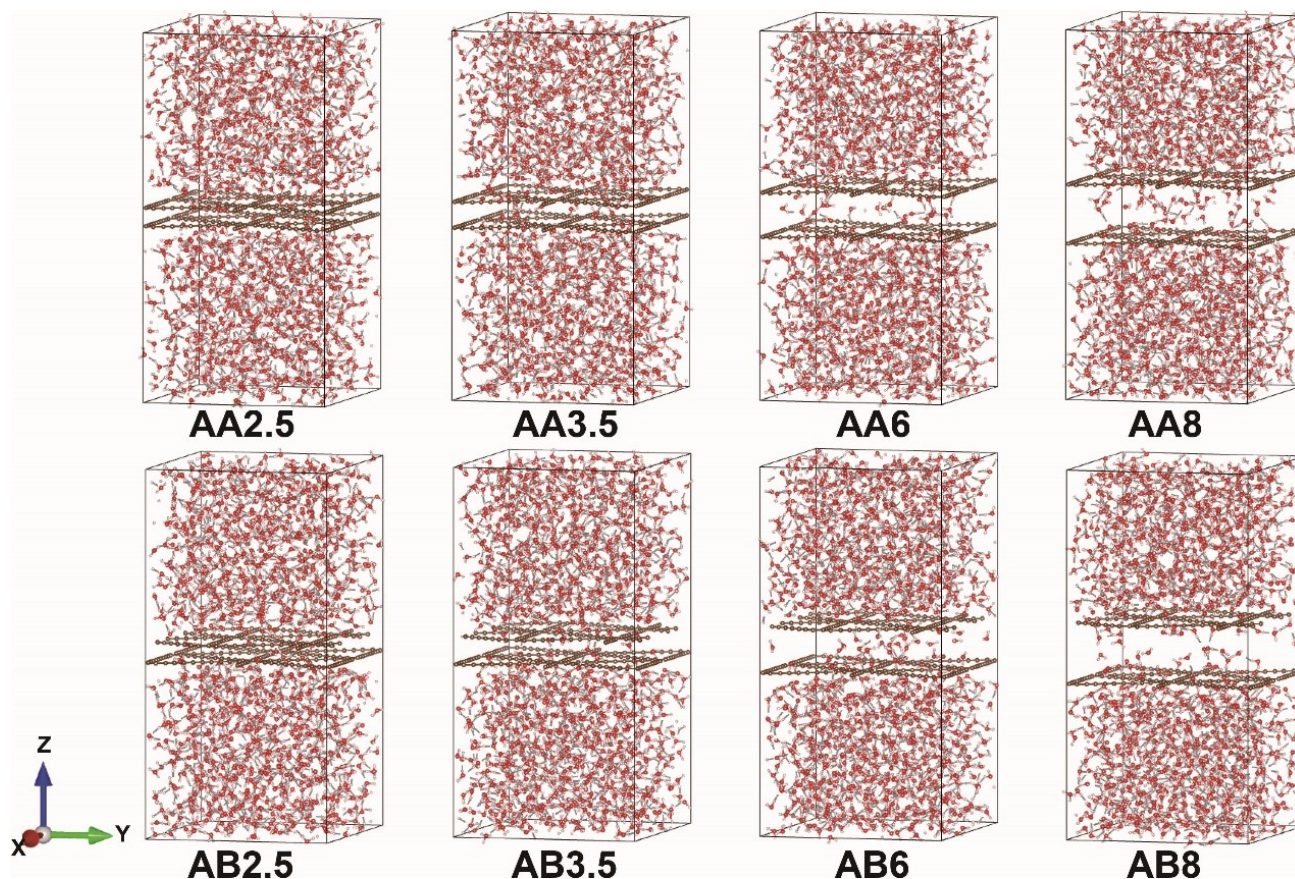


Figure S2 Initial double-layer geometry for NPT process

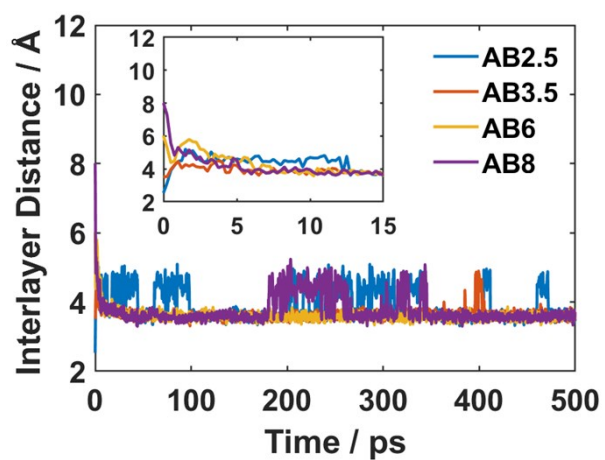


Figure S3 Trajectory of interlayer distance for AB stacked cases in NPT ensemble. The data were collected from 500ps MD simulations.

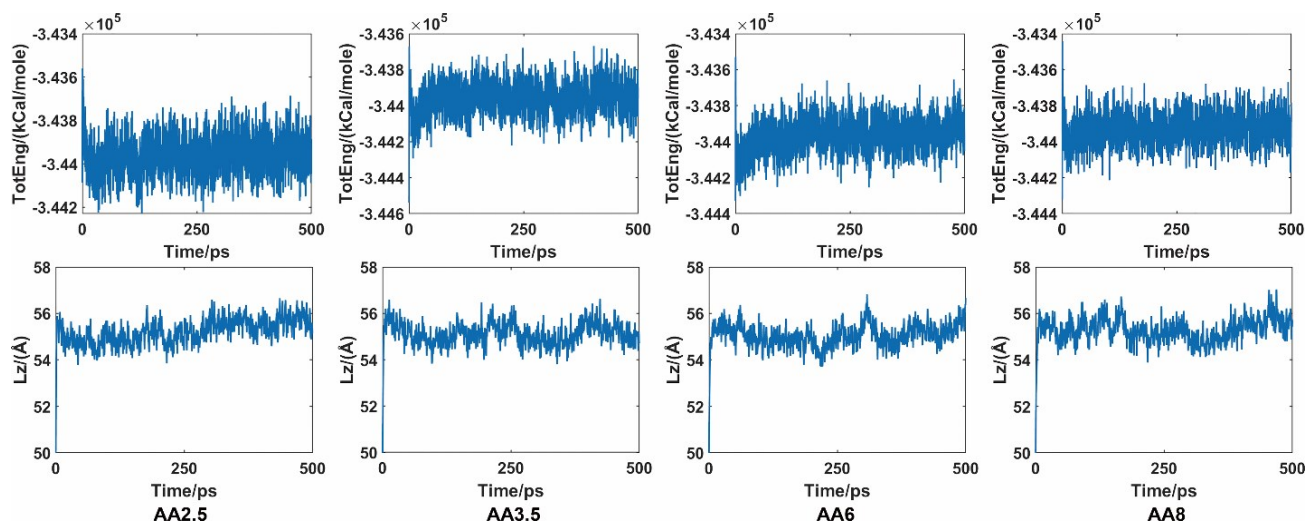


Fig S4 Total Energy and simulation box length in z axis of AA-stacked cases during 500ps NPT process.

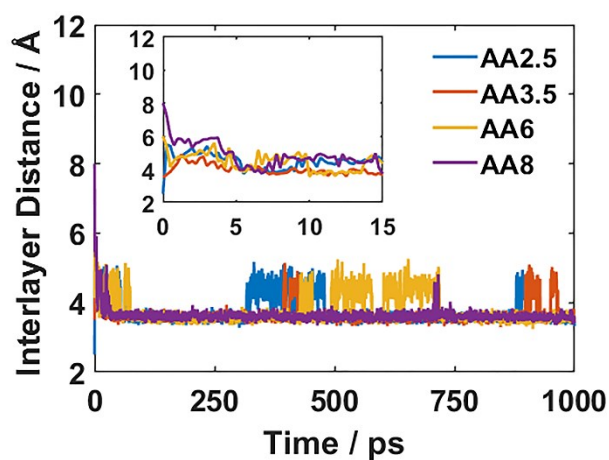


Fig S5 Interlayer distance between the adjacent G4 during 1000ps NPT process.

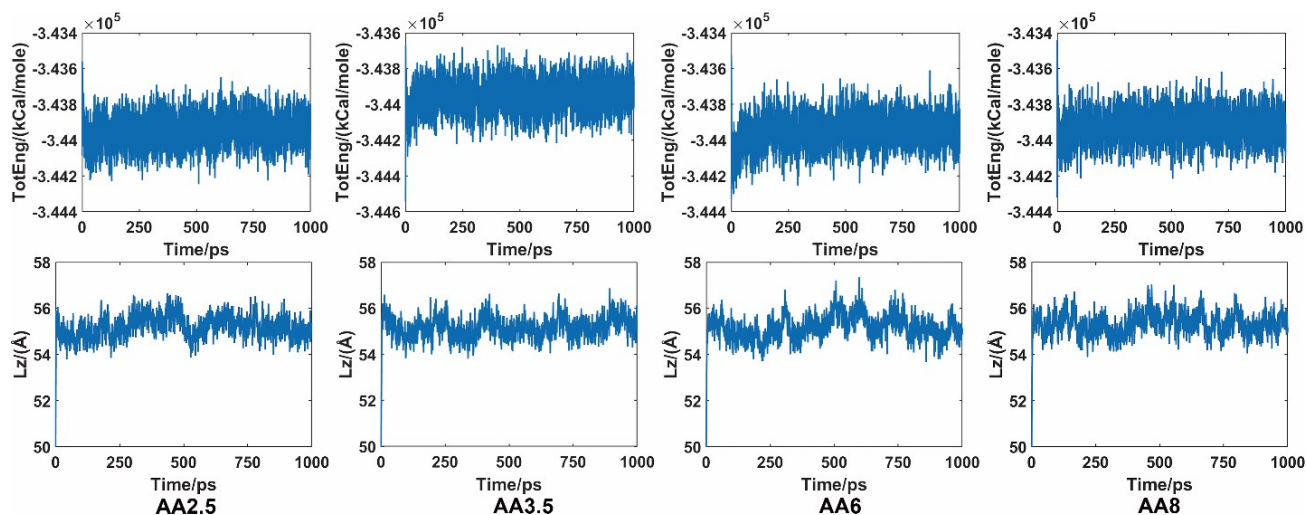


Fig S6 Total Energy and simulation box length in z axis of AA-stacked cases during 1000ps NPT process.

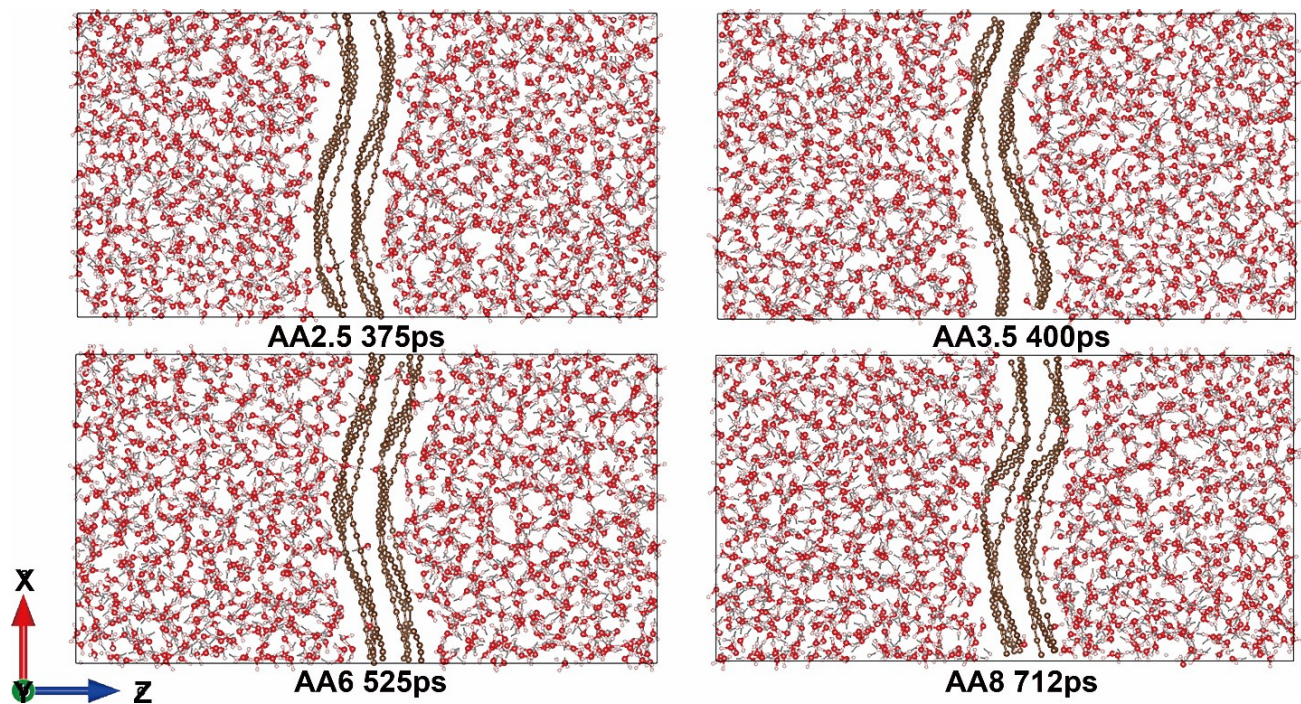


Fig S7 Snapshots from fluctuation periods in Fig S5.

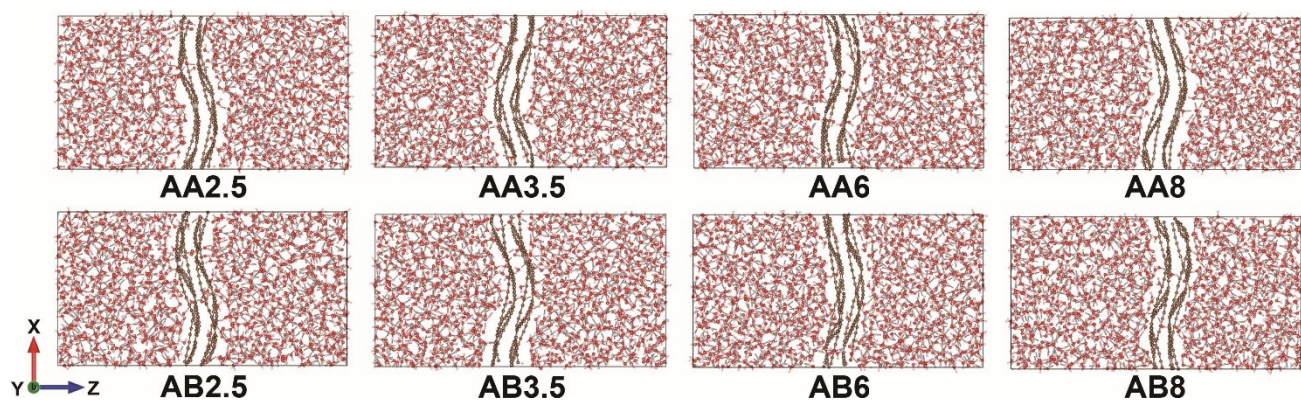


Figure S8 Double-layer geometry after NPT process.



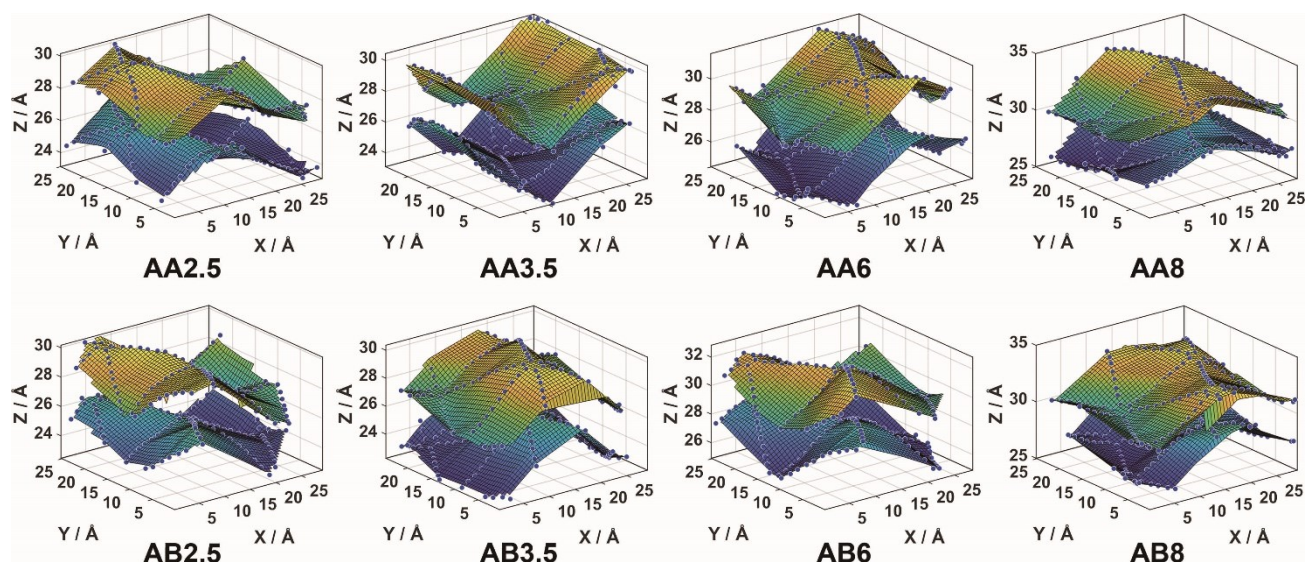


Figure S9 Surface fitting for double-layer G4s in last frame of NPT

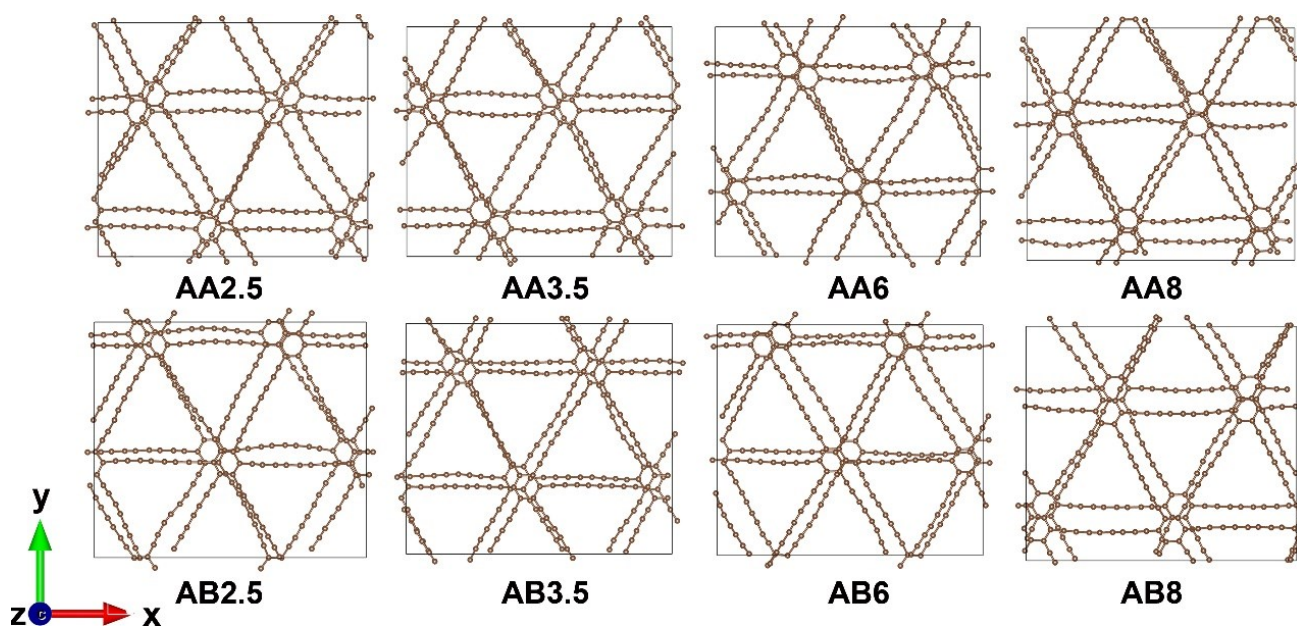


Figure S10 Double-layer G4s' geometry in z direction after NPT process

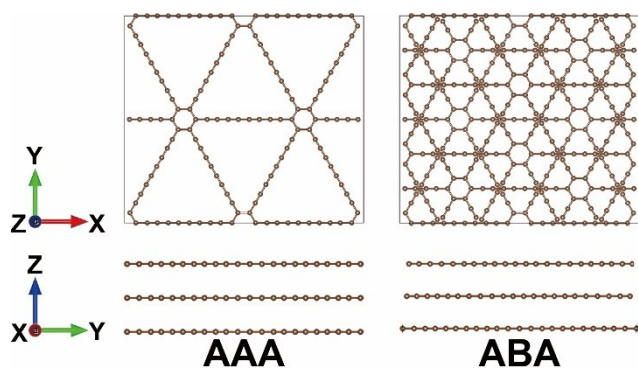


Figure S11 Initial stack geometry of triple-layer G4

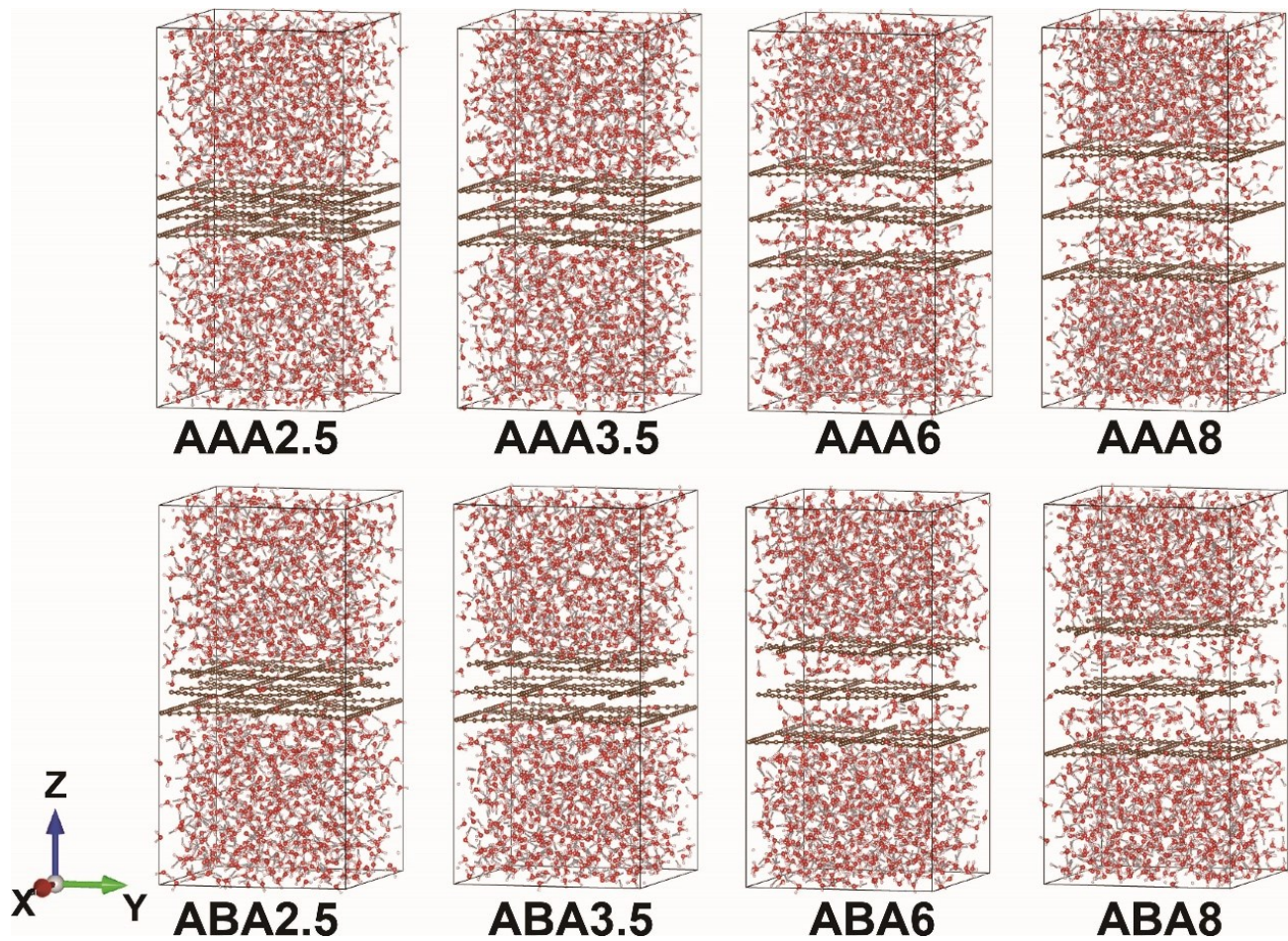


Figure S12 Initial triple-layer geometry for NPT process

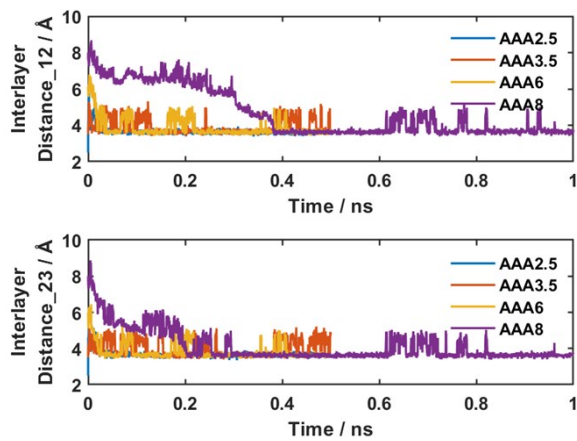


Figure S13 Trajectory of interlayer distance for AAA stacked cases in NPT ensemble. The data were collected from 1ns MD simulations.

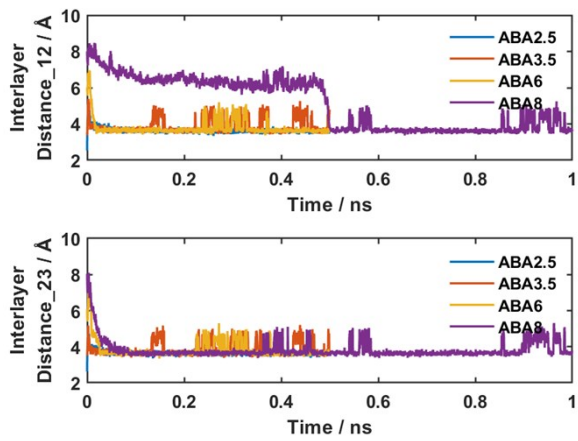


Figure S14 Trajectory of interlayer distance for ABA stacked cases in NPT ensemble. The data were collected from 1ns MD simulations.

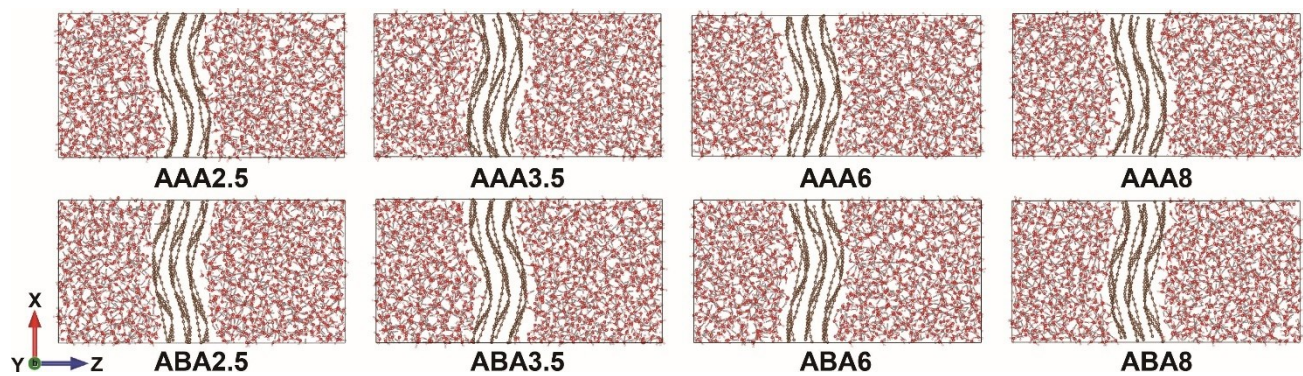


Figure S15 Triple-layer geometry after NPT process.

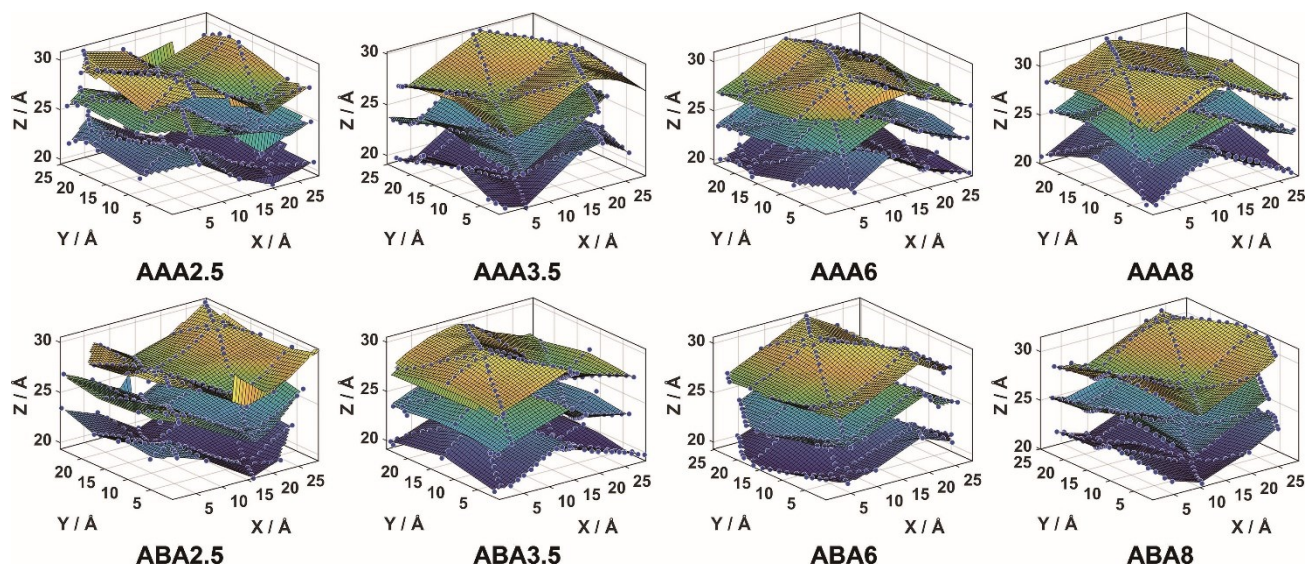


Figure S16 Surface fitting for triple-layer G4s in last frame of NPT

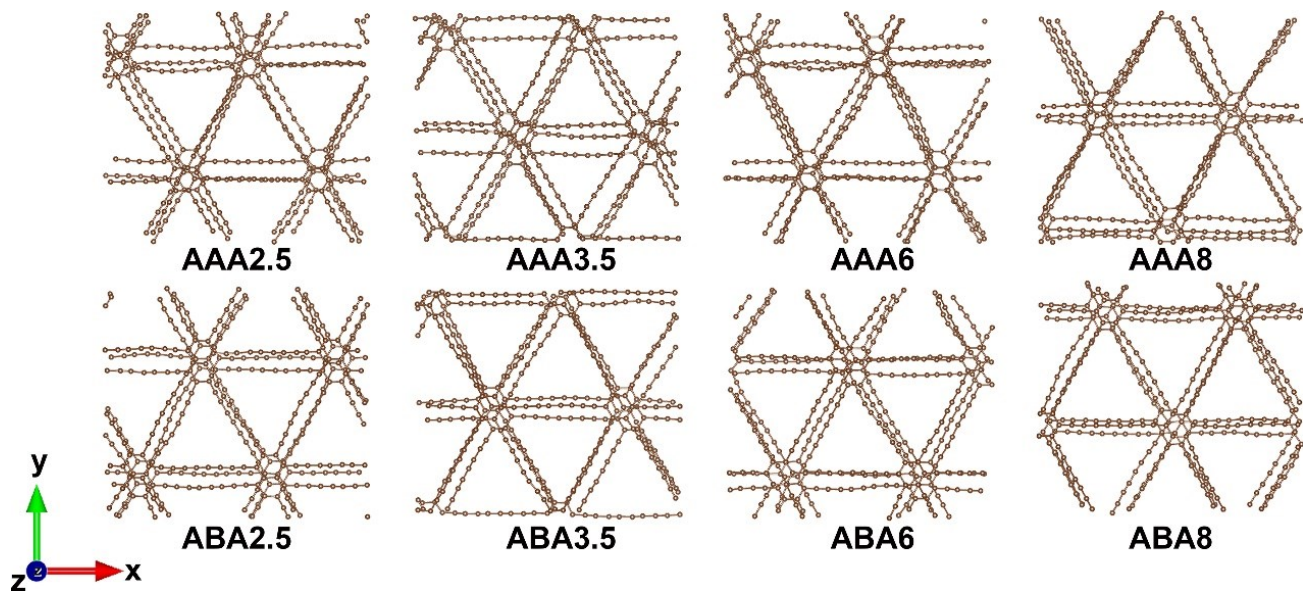


Figure S17 Triple-layer G4s geometry after NPT process

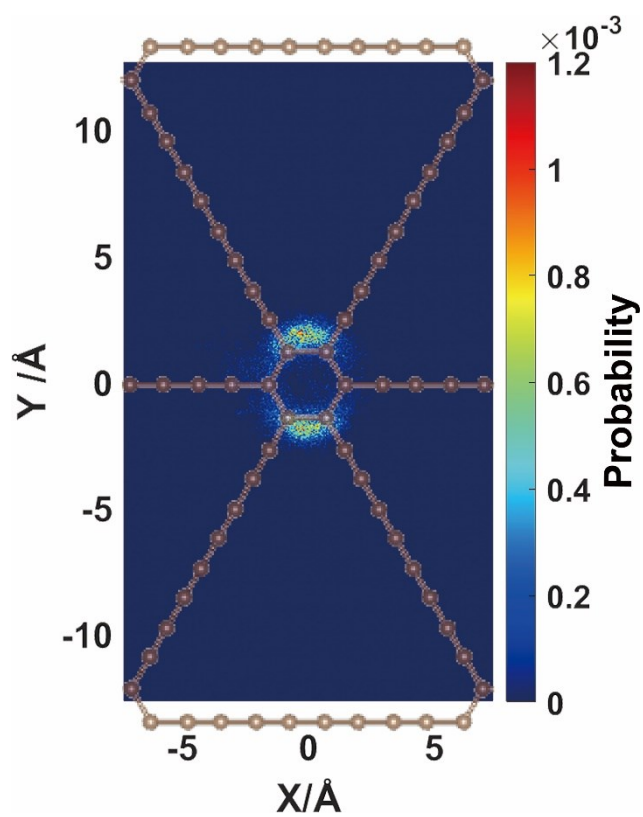


Figure S18 Statistic distribution of misplacement of adjacent G4s in x and y direction from triple-layer cases

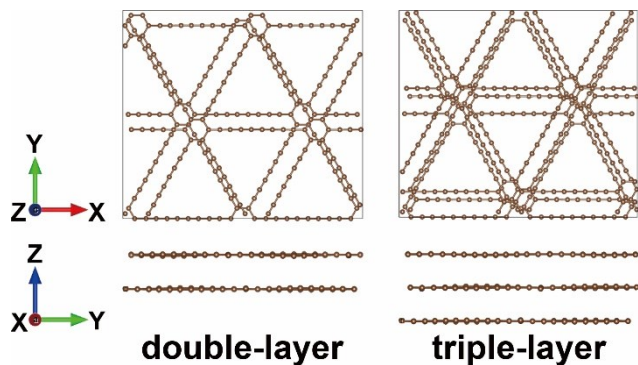


Figure S19 Multilayer G4s after DFT optimization.

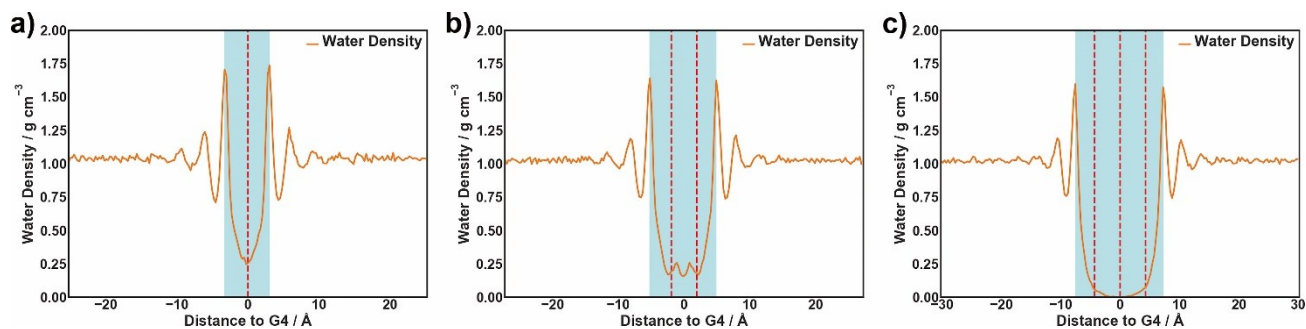


Figure S20 Interfacial area for hydrogen bond analysis

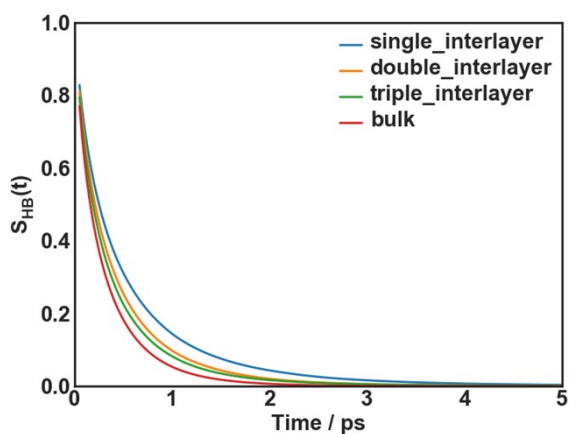


Figure S21 Time dependence of the continuous hydrogen bond correlation functions for hydrogen bonds in cases with different number of G4 layers. The data were collected from MD simulations.

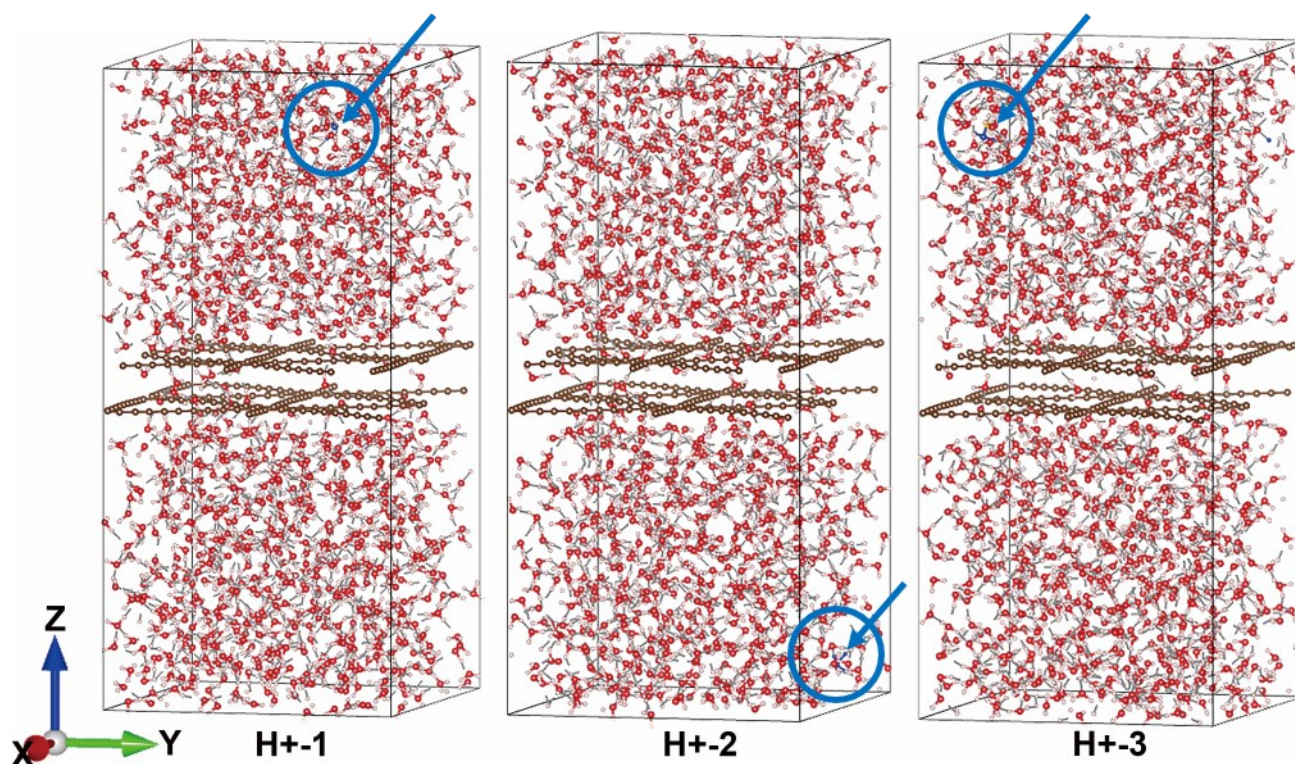


Fig S22 Initial position of hydronium ion in the simulation system. The hydronium ion is plotted in blue.

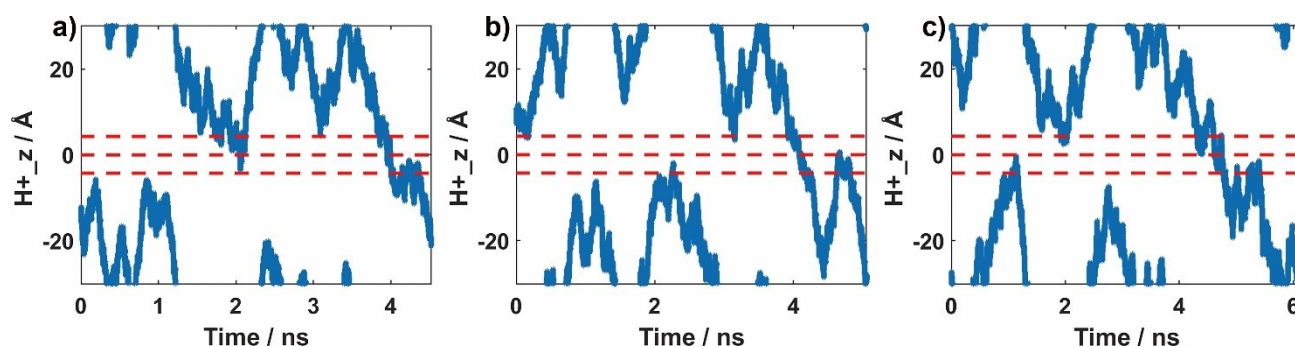


Figure S23 Trajectory of proton during metadynamics process. Three different samples with randomly added proton were simulated. Red lines indicate the position of G4s. The simulation ended at the first traversal of proton along  $z$  axis.<sup>1</sup>

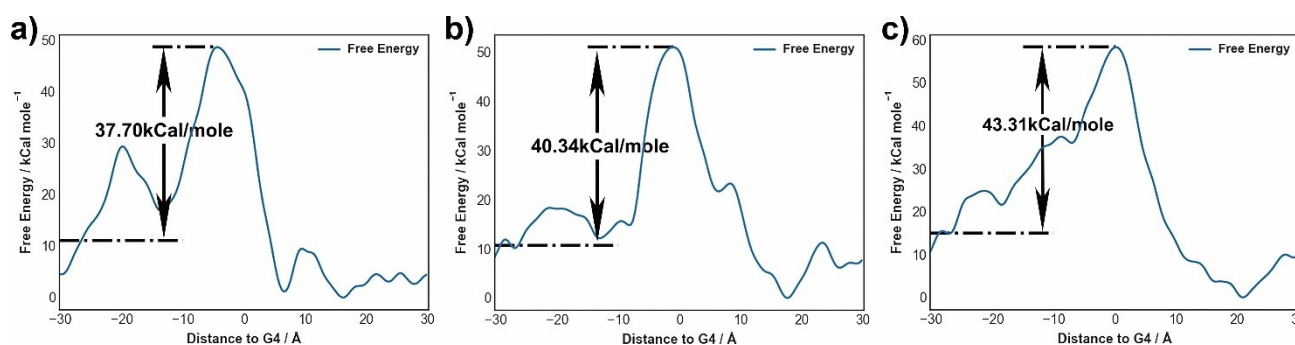


Figure S24 Proton penetration barrier through triple-layer G4. The result is calculated by metadynamics simulations.

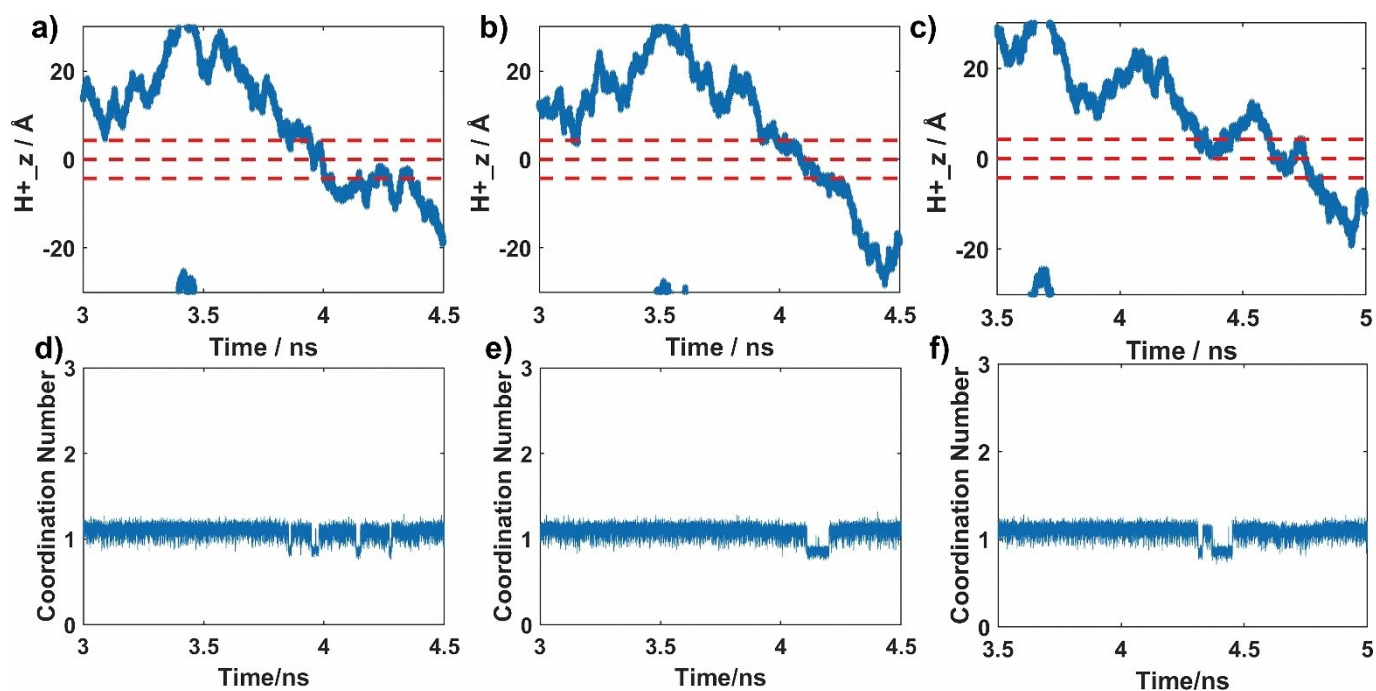


Figure S25 H-O coordination number of the proton in three samples during the penetration period in metadynamics simulations. The results indicate the proton exists as hydronium ion when the penetration happens.

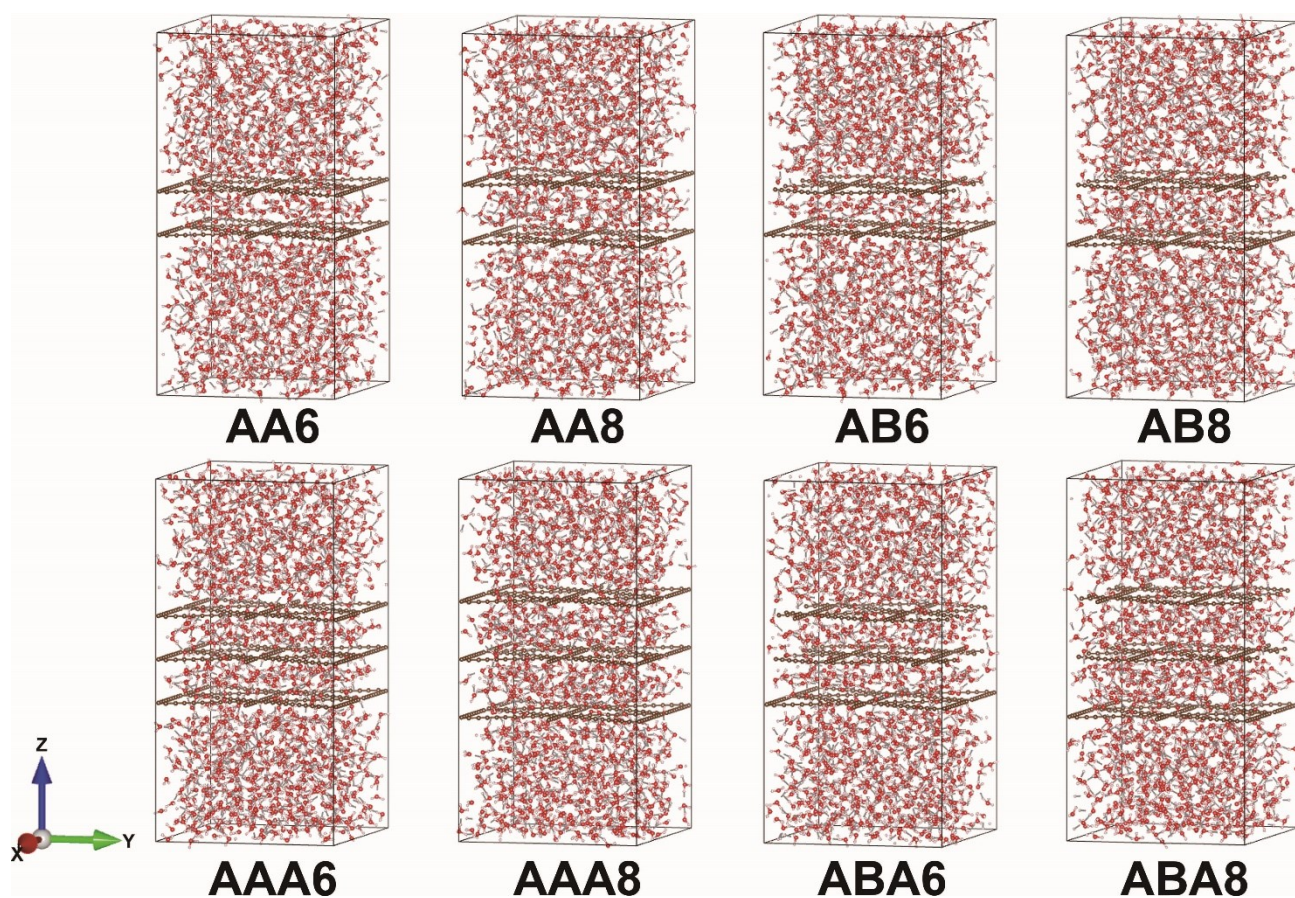


Figure S26 Initial geometry for NPT process with more interlayer water

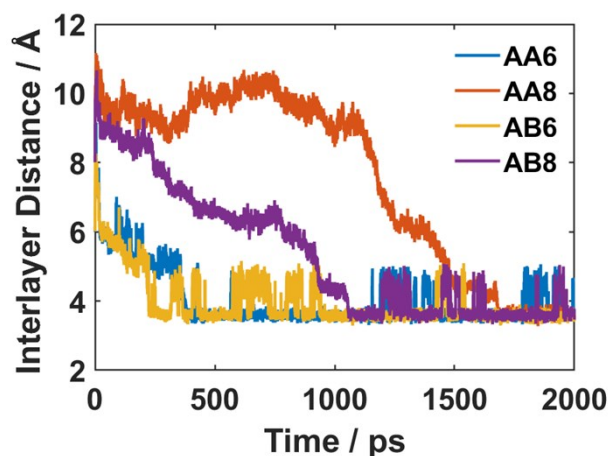


Figure S27 Trajectory of interlayer distance for double-layer cases with more interlayer water molecules in NPT ensemble. The data were collected from 2ns MD simulations.

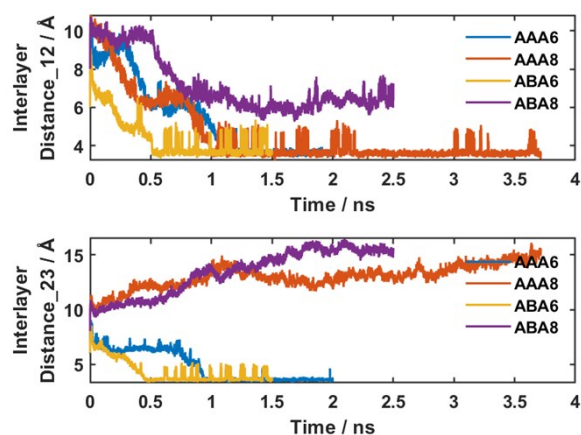


Figure S28 Trajectory of interlayer distance for triple-layer cases with more interlayer water molecules in NPT ensemble. The data were collected from 4ns MD simulations.

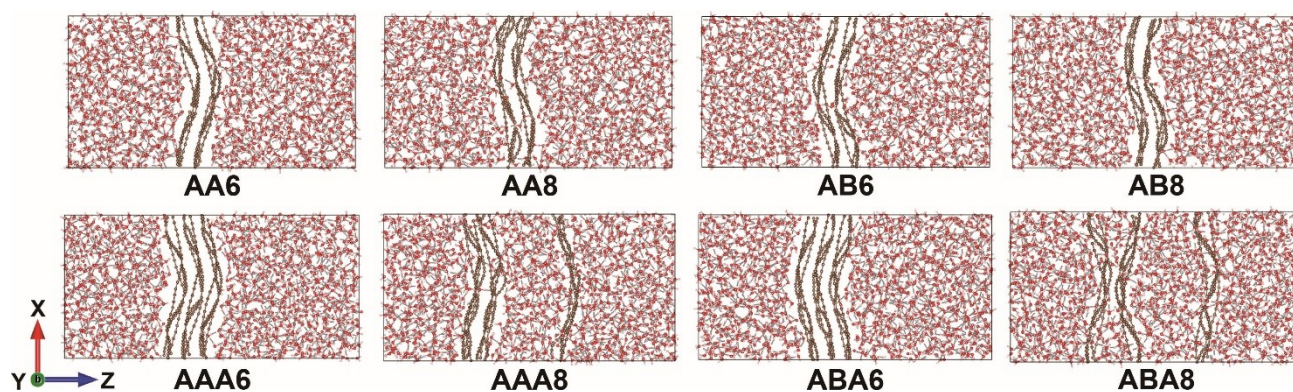


Figure S29 Cases with more interlayer water after NPT process

## Reference

- [S1] A. Barducci, M. Bonomi and M. Parrinello, *WIREs Computational Molecular Science*, 2011, **1**, 826-843.